BNL-79567-2007-CP

QCD Spin Physics in Hadronic Interactions

Werner Vogelsang[1]
[1]Nuclear Theory Group, Physics Dept., Brookhaven National Laboratory, Upton, NY 11973 USA

Presented at the Varenna School on Strangeness and Spin in Fundamental Physics
Varenna, Italy
June 19 to 29, 2007

Physics Department
Nuclear Theory Group

Brookhaven National Laboratory
P.O. Box 5000
Upton, NY 11973-5000
www.bnl.gov

DISCLAIMER

QCD Spin Physics in Hadronic Interactions

Werner Vogelsang

Physics Department, Brookhaven National Laboratory, Upton, NY 11973

Summary. — We discuss spin phenomena in high-energy hadronic scattering, with a particular emphasis on the spin physics program now underway at the first polarized proton-proton collider, RHIC. Experiments at RHIC unravel the spin structure of the nucleon in new ways. Prime goals are to determine the contribution of gluon spins to the proton spin, to elucidate the flavor structure of quark and antiquark polarizations in the nucleon, and to help clarify the origin of transverse-spin phenomena in QCD. These lectures describe some aspects of this program and of the associated physics.

1. – Introduction

For many years now, spin has played a very prominent role in QCD. The field of QCD spin physics has been driven by the hugely successful experimental program of polarized deeply-inelastic lepton-nucleon scattering (DIS) [1]. One of the most important results of this program has been the finding that the quark and anti-quark spins (summed over all flavors) provide only about a quarter of the nucleon's spin, $\Delta\Sigma \approx 0.25$ in the proton helicity sum rule [2]

$$\frac{1}{2} = \frac{1}{2}\Delta\Sigma(Q^2) + \Delta G(Q^2) + L_q(Q^2) + L_g(Q^2) \,, \tag{1}$$

implying that sizable contributions to the nucleon spin should come from the gluon spin contribution $\Delta G(Q^2)$, or from orbital angular momenta $L_{q,g}(Q^2)$ of partons. Here, Q is the resolution scale at which one probes the nucleon.

To determine the gluon spin contribution on the right-hand-side of eq. (1) has become a major focus of the field. Like $\Delta\Sigma$, it can be probed in polarized high-energy scattering. Several current experiments are dedicated to a direct determination of the spin-dependent gluon distribution $\Delta g(x, Q^2)$,

$$\Delta g(x, Q^2) \equiv g^+(x, Q^2) - g^-(x, Q^2) \ , \tag{2}$$

where g^+ (g^-) denotes the number density of gluons in a longitudinally polarized proton with same (opposite) sign of helicity as the proton's, and where x is the gluon's light-cone momentum fraction. The field-theoretic definition of Δg is

$$\Delta g(x, Q^2) = \frac{i}{4\pi\, x\, P^+} \int d\lambda\, e^{i\lambda x P^+} \, \langle P, S | G^{+\nu}(0)\, \tilde{G}^{+}{}_{\nu}(\lambda n) | P, S\rangle \Big|_{Q^2} \ , \tag{3}$$

written in $A^+ = 0$ gauge. $G^{\mu\nu}$ is the QCD field strength tensor, and $\tilde{G}^{\mu\nu}$ its dual. The integral of $\Delta g(x, Q^2)$ over all momentum fractions x becomes a local operator only in $A^+ = 0$ gauge and then coincides with $\Delta G(Q^2)$ [2, 3, 4]. The COMPASS experiment at CERN and the HERMES experiment at DESY attempt to access $\Delta g(x, Q^2)$ in charm- or high-p_T hadron final states in photon-gluon fusion $\gamma^* g \to q\bar{q}$ [5, 6]. A new milestone has been reached with the advent of the first polarized proton-proton collider, RHIC at BNL [7, 8, 9]. By colliding longitudinally polarized protons at high energies, RHIC will provide precise and detailed information on Δg, over a wide range of x and Q^2, and from a variety of probes.

There are also important spin phenomena in QCD associated with transversely polarized high-energy nucleons [10, 11]. Single-transverse spin asymmetries (SSAs), in particular, play an important role for our understanding of QCD and of nucleon structure. They have a long history, starting from the 1970s and 1980s when surprisingly large SSAs were observed in hadronic reactions such as $p^\uparrow p \to \pi X$ at forward angles of the produced pion [12]. The last few years have seen a renaissance in the experimental studies of SSAs. The HERMES collaboration at DESY, SMC and COMPASS at CERN, and the CLAS collaboration at the Jefferson Laboratory have investigated SSAs in semi-inclusive hadron production $eN^\uparrow \to e\pi X$ in deep-inelastic scattering [13]. For proton targets, remarkably large asymmetries were found. With the advent of RHIC, there are new possibilities for extending the studies of SSAs in hadronic scattering into a regime where the use of QCD perturbation theory in the analysis of the data appears to be justified.

These lectures discuss some of the most important aspects of high-energy polarized pp scattering at RHIC. We will start out with a brief synopsis of perturbative QCD and its applications in hadronic scattering. We will then discuss separately the physics associated with longitudinally and transversely polarized pp collisions.

2. – QCD perturbation theory and its applications

The prerequisite for many of our efforts to study the inner structure of the nucleon is the "asymptotic freedom" of QCD [14]. This term describes the property of the strong coupling constant α_s to decrease with increasing momentum transfer (or towards shorter distances):

$$\alpha_s(Q^2) = \frac{\alpha_s(\mu^2)}{1 + \frac{\alpha_s(\mu^2)}{12\pi}(33 - 2n_f)\log\left(\frac{Q^2}{\mu^2}\right)}, \tag{4}$$

where n_f is the number of quark and anti-quark flavors. Because of asymptotic freedom, it should be possible to use perturbation theory in terms of the quarks and gluons of QCD when the momentum transfer is sufficiently high. Indeed, despite the fact that ultimately all strong interaction phenomena will also involve hadronic mass scales and hence the confinement regime of QCD, QCD perturbation theory has turned out to be highly useful and successful for quantities that are either

- insensitive to details of long-distance physics at leading power in momentum transfer (infrared-safe),

or

- for which short-distance and (non-perturbative) long-distance phenomena may be separated ("factorized") from one another.

In the following, let us discuss examples of both.

2·1. *Perturbative QCD in e^+e^- annihilation*. – The simplest QCD observable in e^+e^- annihilation is the fully inclusive total cross section for $e^+e^- \to$ hadrons. At sufficiently high center-of-mass energy s, a first-order approximation to this cross section is given by that for $e^+e^- \to q\bar{q}$, with massless quarks, which is

$$\sigma_{e^+e^-\to q\bar{q}} \equiv \sigma_0 = \frac{4\pi\alpha^2}{3s} N_c \sum_{q=u,d,s,\ldots} e_q^2, \tag{5}$$

where $N_c = 3$ is the number of colors in QCD and e_q denotes the quark fractional electromagnetic charge. Once the q and $\bar{q}$ have been produced in the collision, they will hadronize, which is certainly a non-perturbative process. However, the cross section we are considering is totally inclusive, that is, we sum over *all* hadronic final states. The total probability for the q and $\bar{q}$ to turn into some hadronic final state is unity, which is the reason why σ_0 is a useful first-order approximation. What happens at higher orders in perturbation theory? At the next order, $\mathcal{O}(\alpha_s)$, one needs to consider virtual loop corrections to $e^+e^- \to q\bar{q}$ (interfering with the lowest-order process), as well as real-gluon emission from one of the outgoing quark legs. Both these contributions are separately infinite. For example, the real-emission diagrams become singular when the gluon is radiated parallel to one of the outgoing quark lines, or when it becomes very soft. The same happens in the virtual diagrams. These singularities signal the onset of long-distance physics. However, the sum of real and virtual diagrams is finite, giving rise to a moderate correction to the perturbative cross section:

$$\sigma_{e^+e^-\to\,\mathrm{hadrons}} = \sigma_0 \left[1 + \frac{\alpha_s}{\pi}\right] . \tag{6}$$

Let us take stock. We have found a perturbative way of calculating the cross section for $e^+e^- \to$ hadrons. We do this by calculating "$e^+e^- \to$ strongly interacting particles" at the level of the quarks and gluons of QCD. The reason why this can be done is precisely that we have considered a cross section that is insensitive to details of long-distance physics. We have not asked for the cross section for producing, say, five low-energy pions at certain angles, but rather a cross section that collects *all* hadronic final states, no matter how they were eventually generated in the hadronization mechanism. For such long-distance-insensitive observables QCD perturbation theory is useful. At the level of quarks and gluons, insensitivity to long-distance physics means that the observable is defined in such a way that it does not change if a final-state quark or gluon collinearly splits into a pair, or if a final-state particle becomes very soft. Such observables are referred to as "infrared-safe" (IR-safe).

The perturbative cross section for $e^+e^- \to$ hadrons is

$$\sigma_{e^+e^-\to\,\mathrm{hadrons}} = \sigma_0 \left[1 + \alpha_s(s)\, c_1 + \alpha_s^2(s)\, c_2 + \ldots\right] \tag{7}$$

with coefficients c_i. Corrections to this formula as such are of non-perturbative nature and suppressed by inverse powers of s. That such "power-corrections" occur may for example be seen by keeping a finite quark mass m_q in the calculation of the lowest-order cross section σ_0, in which case

$$\sigma_0 = \frac{4\pi\alpha^2}{3s} N_c \sum_{q=u,d,s,\ldots} e_q^2 \sqrt{1-\frac{4m_q^2}{s}} \left(1+\frac{2m_q^2}{s}\right) \approx \frac{4\pi\alpha^2}{3s} N_c \sum_{q=u,d,s,\ldots} e_q^2 \left[1+\mathcal{O}\left(\frac{m_q^4}{s^2}\right)\right] . \tag{8}$$

If $m_q \ll \Lambda_{\mathrm{QCD}}$, it will set a non-perturbative mass scale. The power suppression of non-perturbative effects by two powers (or more) of s is actually generic in $e^+e^- \to$ hadrons.

The total cross section for $e^+e^- \to$ hadrons is the simplest example of an "infrared-safe" (IR-safe) observable. It was discovered that there are many other IR-safe observables in e^+e^- annihilation. A classic IR safe observable are the "Sterman-Weinberg jets" [15]. An event in e^+e^- annihilation qualifies as a Sterman-Weinberg jet event if one can find two oppositely directed cones of half-opening δ so that all hadronic energy except a fraction $\epsilon\sqrt{s}$ is inside these cones. This observable has been the progenitor of all jet observables in QCD.

2·2. *Factorized deep-inelastic scattering* . – For our purposes, factorized cross sections are particularly interesting. These are not *per se* IR-safe, but allow a separation of long-distance from short-distance phenomena. The classic example is the cross section (or structure function) for deep-inelastic scattering (DIS). At large momentum transfer Q^2, a DIS structure function may be written in the simple parton model as

$$F_{\rm DIS} = \int_x^1 \frac{d\xi}{\xi}\, q(\xi)\, \hat{F}(x/\xi) \; , \tag{9}$$

where q is the quark parton distribution (we assume here that we have only one quark flavor) and $\hat{F}$ is the partonic structure function describing the scattering of the virtual DIS photon off the quark. The parton model has the notion of a separation of long-distance (q) from short-distance ($\hat{F}$) effects. How does this hold up in QCD? One finds that this separation can be proven systematically to all orders, resulting schematically in

$$F_{\rm DIS}\left(\frac{Q}{\lambda}\right) = q\left(\frac{\mu}{\lambda}, \alpha_s(\mu)\right) \otimes \hat{F}\left(\frac{Q}{\mu}, \alpha_s(\mu)\right) + \mathcal{O}\left(\frac{\kappa^2}{Q^2}\right) \; , \tag{10}$$

where $\otimes$ denotes the integral convolution in x given in (9). Here λ denotes generically a non-perturbative mass scale. All dependence on λ is in the quark distribution function, whereas all dependence on the hard scale Q resides in $\hat{F}$. However, this factorization implies the presence of a "factorization scale" μ. This scale may be thought of as the scale that distinguishes when contributions are to be absorbed into the quark distribution or into the partonic structure function, respectively. Corrections to the factorized form in eq. (10) are suppressed by inverse powers of Q^2 and become negligible at high Q^2.

Physics of course should be independent of the choice of μ. This requirement leads to the scale evolution of parton distribution functions. For the helicity distributions, for example, the evolution equations [16, 17] read

$$\frac{\rm d}{{\rm d}\ln\mu^2}\begin{pmatrix}\Delta q\\ \Delta g\end{pmatrix}(x,\mu^2) = \begin{pmatrix}\Delta P_{qq}(\alpha_s(\mu),x) & \Delta P_{qg}(\alpha_s(\mu),x)\\ \Delta P_{gq}(\alpha_s(\mu),x) & \Delta P_{gg}(\alpha_s(\mu),x)\end{pmatrix} \otimes \begin{pmatrix}\Delta q\\ \Delta g\end{pmatrix}(x,\mu^2) \; , \tag{11}$$

where the ΔP_{ij} are known as "splitting functions" [17, 18, 19] and are evaluated in QCD perturbation theory. Evolution resums collinear logarithms of the form $\alpha_s^k \ln(Q/Q_0)^m$ ($m \le k$) between the initial scale Q_0 for the parton distributions and the hard scale Q.

2·3. *Factorized pp scattering* . – Factorization is the basic concept that underlies most of RHIC spin physics [20]. Like for DIS, cross sections for large-momentum-transfer reactions in pp scattering may be factorized into long and short-distance contributions. The long-distance pieces contain information on the structure of the nucleon in terms of its distributions of constituents, "partons". The short-distance parts describe the hard interactions of these partons and can be calculated from first principles in QCD perturbation theory. While the parton distributions describe universal properties of the nucleon, that is, are the same in each reaction, the short-distance parts carry the process-dependence and have to be calculated for each reaction considered. The factorization just described for the case of DIS is the prototype.

As an explicit example in pp scattering, we consider the cross section for the reaction $pp \to \pi(p_T)X$, where the pion is at high transverse momentum p_T, ensuring large momentum transfer. X denotes an arbitrary hadronic final state, which is summed over. The statement of the factorization theorem is then:

$$d\sigma = \sum_{a,b,c} \int dx_a \int dx_b \int dz_c \;\; f_a(x_a,\mu) \;\; f_b(x_b,\mu)\, D_c^{\pi}(z_c,\mu)$$
$$\times\, d\hat{\sigma}_{ab}^{c}(x_a P_A, x_b P_B, P_\pi/z_c, \mu) \;\; , \tag{12}$$

where the sum is over all contributing partonic channels $a + b \to c + X$, with $d\hat{\sigma}_{ab}^{c}$ the associated partonic cross section. The $f_{a,b}$ describe the distributions of partons in the nucleon. In this particular example, the fact that we are observing a specific hadron in the reaction requires the introduction of additional long-distance functions, the parton-to-pion fragmentation functions D_c^{π}. These functions have been determined with some accuracy by observing leading pions in e^+e^- collisions and in DIS [21]. As we discussed above, a factorization of a physical quantity into contributions associated with different length scales will rely on a "factorization" scale that defines the boundary between what is referred to as "short-distance" and "long-distance". The dependence on the value of μ decreases order by order in perturbation theory. This is a reason why knowledge of higher orders in the perturbative expansion of the partonic cross sections is important. We recall that eq. (12) is of course not an exact statement. There are corrections to eq. (12) that are down by inverse powers of the momentum transfer, the so-called "power corrections". These corrections may become relevant towards lower p_T. As we shall see below, comparisons of RHIC data for unpolarized cross sections with theoretical calculations based on eq. (12) do not suggest that power corrections play a very significant role in the RHIC kinematic regime, even down to fairly low p_T.

Figure 1 offers a graphic illustration of QCD factorization. Thanks to factorization, one can study nucleon structure, represented by the parton densities $f_{a,b}(x,\mu)$, through a measurement of $d\sigma$, hand in hand with a theoretical calculation of $d\hat{\sigma}$. The latter may be evaluated in QCD perturbation theory. Schematically, they can be expanded as

$$d\hat{\sigma}_{ab}^{c} \;=\; d\hat{\sigma}_{ab}^{c,(0)} + \frac{\alpha_s}{\pi} d\hat{\sigma}_{ab}^{c,(1)} + \ldots \;. \tag{13}$$

$d\hat{\sigma}_{ab}^{c,(0)}$ is the leading-order (LO) approximation to the partonic cross section. The lowest order can generally only serve to give a rough description of the reaction under study. It merely captures the main features, but does not usually provide a quantitative understanding. The first-order ("next-to-leading order" (NLO)) corrections are usually indispensable in order to arrive at a firmer theoretical prediction for hadronic cross sections.

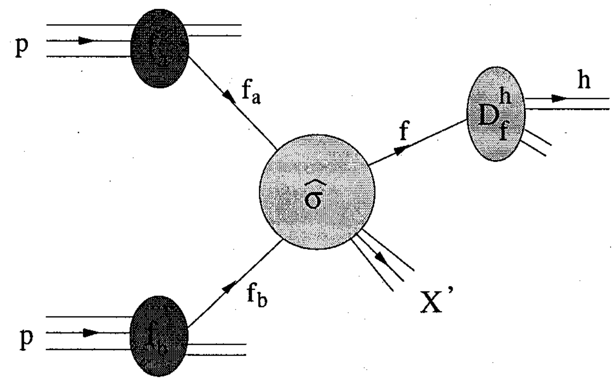

Fig. 1. – *Factorization of* $pp \to \pi^0 X$ *in terms of parton densities, partonic hard-scattering cross sections, and fragmentation functions.*

We emphasize that the factorization in eq. (12) involves integrations over the partons' momentum fractions $x_{a,b}, z_c$ only, which appear in the relations between the partonic and hadron momenta, $p_a = x_a P_a$ in the initial state and $p_c = P_\pi / z_c$ in the final state. Such a factorization is known as "collinear" factorization. It applies in particular to single-inclusive reactions such as $pp \to \pi X$.

3. – Longitudinally polarized pp collisions at RHIC

3·1. *Results from unpolarized pp scattering at RHIC* . – There have already been results from RHIC that demonstrate that the NLO framework is very successful. This is shown by fig. 2 which presents comparisons of data from PHENIX and STAR for mid-rapidity π^0 [22] and jet [23], forward π^0 [24], and mid-rapidity direct-photon [25] production with NLO calculations [26, 27, 28, 29, 30, 31]. This provides the basis for extending this type of analysis to polarized reactions. In addition, each of the cross sections shown are strongly dominated by partonic scatterings with initial gluons [8]. As an example, in fig. 3 we decompose the NLO mid-rapidity π^0 cross section into the relative contributions from the various two-parton initial states. It is evident that qg and gg scattering dominate.

3·2. *Probing the spin structure of the nucleon in polarized pp collisions.* – The measured quantities in spin physics experiments at RHIC are *spin asymmetries.* For collisions of longitudinally polarized proton beams, one defines a double-spin asymmetry for a given process by

$$A_{LL} = \frac{d\sigma(++) - d\sigma(+-)}{d\sigma(++) + d\sigma(+-)} \equiv \frac{d\Delta\sigma}{d\sigma} , \tag{14}$$

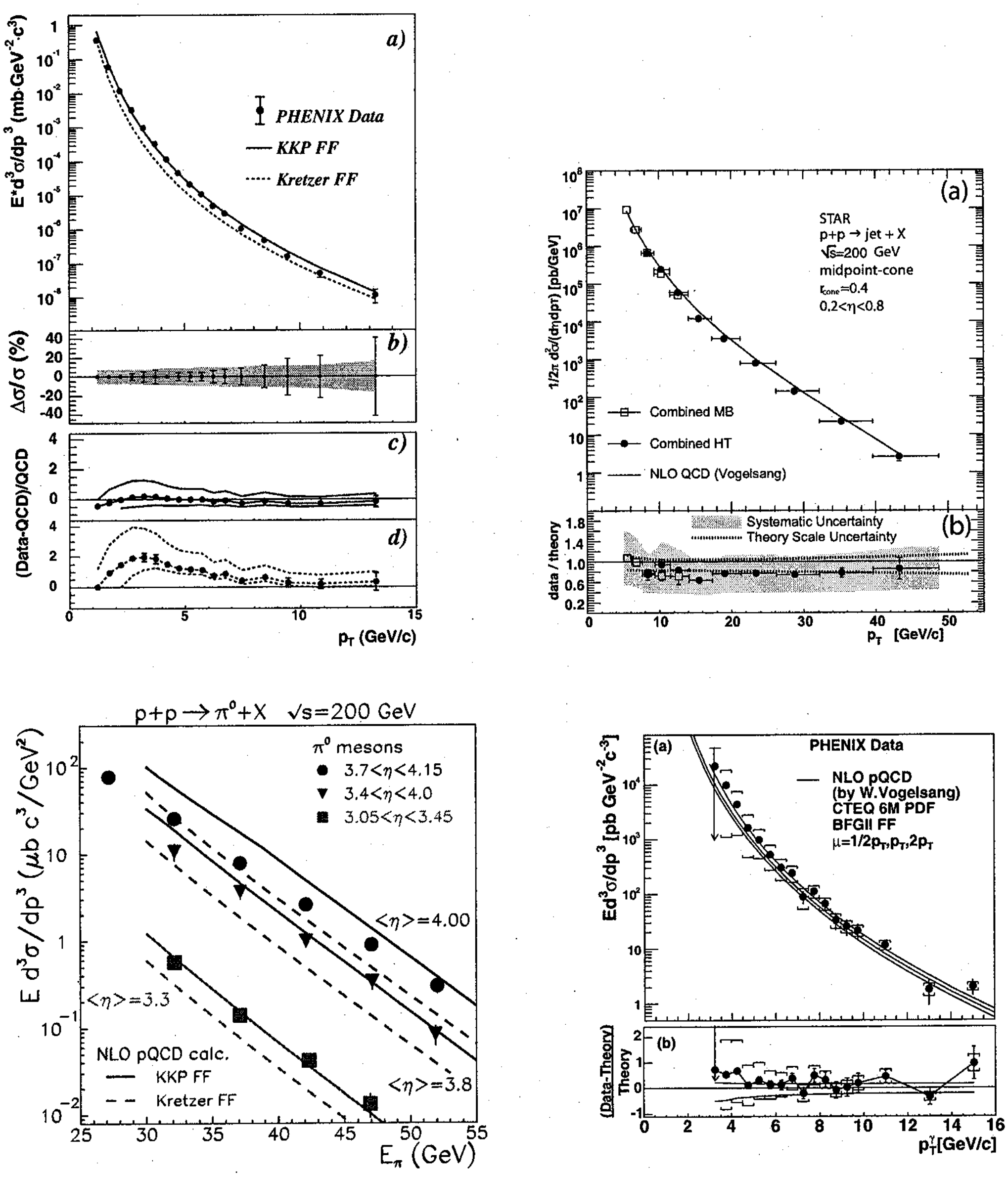

Fig. 2. – Data for the cross section for single-inclusive π^0 production $pp \to \pi^0 X$ at $\sqrt{s} = 200$ GeV at mid-rapidity from PHENIX (upper left, [22]) and at forward rapidities from STAR (lower left, [24]), for mid-rapidity jet production from STAR (upper right, [23]), and for mid-rapidity prompt-photon production from PHENIX (lower right, [25]). The lines show the results of the corresponding next-to-leading order calculations [28, 29, 31].

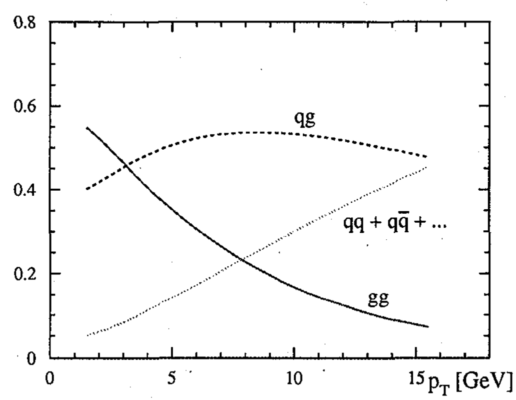

Fig. 3. – Relative contributions to the mid-rapidity NLO cross section for $pp \to \pi^0 X$ at $\sqrt{s} =$ 200 GeV from gg, qg, and qq initial states [8].

where the signs indicate the helicities of the incident protons. The basic concepts laid out so far for unpolarized inelastic pp scattering carry over to the case of polarized collisions: spin-dependent inelastic pp cross sections factorize into "products" of polarized parton distribution functions of the proton and hard-scattering cross sections describing spin-dependent interactions of partons. As in the unpolarized case, the latter are calculable in QCD perturbation theory since they are characterized by large momentum transfer. Schematically, one has for the numerator of the spin asymmetry:

$$d\Delta\sigma = \sum_{a,b=q,\bar{q},g} \Delta f_a \otimes \Delta f_b \otimes d\Delta\hat{\sigma}_{ab} \ , \tag{15}$$

where $\otimes$ denotes a convolution and where the sum is over all contributing partonic channels $a+b \to c+X$ producing the desired high-p_T or large-invariant mass final state. $d\Delta\hat{\sigma}_{ab}$ is the associated perturbative spin-dependent partonic cross section, defined as

$$d\Delta\hat{\sigma}_{ab} = \frac{1}{2}\left[d\hat{\sigma}_{ab}(++) - d\hat{\sigma}_{ab}(+-) \right] \ , \tag{16}$$

the signs now denoting the helicities of the initial partons a, b. The sensitivity with which one can probe the polarized parton densities will foremost depend on the weights with which they enter the cross section. Good measures for this are the so-called partonic "analyzing powers". The latter are just the spin asymmetries

$$\hat{a}_{LL} = \frac{d\hat{\sigma}_{ab}(++) - d\hat{\sigma}_{ab}(+-)}{d\hat{\sigma}_{ab}(++) + d\hat{\sigma}_{ab}(+-)} \tag{17}$$

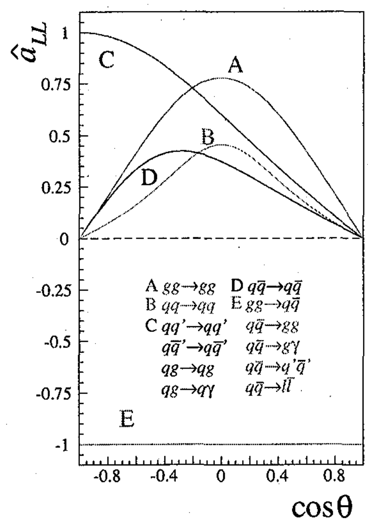

Fig. 4. – *Helicity asymmetries for the most important partonic reactions at RHIC at lowest order in QCD.*

for the individual partonic subprocesses. Figure 4 shows these analyzing powers at LO for all partonic reactions. One can see that they are usually very substantial. As an example, consider $q\bar{q}$ annihilation processes into any number of bosons. Because of helicity conservation at the Standard-Model fermion-boson vertices (for massless quarks), the annihilating quark and anti-quark need to have opposite helicities in order for the reaction to take place, regardless of how many final-state bosons couple to them. Thus all reactions of the type $q\bar{q} \to \gamma^*$, $q\bar{q} \to gg$, $\ldots$, have a partonic analyzing power -1. The same is true for the s-channel process $q\bar{q} \to q'\bar{q}'$, but not for the process $q\bar{q} \to q\bar{q}$ which also has a t-channel contribution.

Since the partonic cross sections are calculable from first principles in QCD, eq. (15) may be used to determine the polarized parton distribution functions from measurements of the spin-dependent pp cross section on the left-hand side. The crucial point here is that, as discussed in the previous section, the parton distributions are universal. They are the same in all inelastic processes, not only in pp scattering, but also for example in deeply-inelastic lepton nucleon scattering which up to now has mostly been used to learn about nucleon spin structure. This means that inelastic processes with polarization have the very attractive feature that they probe fundamental and universal spin structure of the nucleon. In effect, one is using the asymptotically free regime of QCD to probe the deep structure of the nucleon.

At RHIC, there are a number of sensitive and measurable processes. The key ones are listed in Table I, where we also give the dominant underlying partonic reactions and the aspect of nucleon spin structure they probe. We emphasize that, even though we have only shown LO results in fig. 4, the NLO corrections are available for each process

Reaction	Dom. partonic process	probes	LO Feynman diagram
$\vec{p}\vec{p} \to \pi + X$	$\vec{g}\vec{g} \to gg$ $\vec{q}\vec{g} \to qg$	Δg	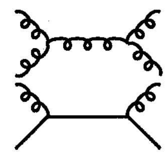
$\vec{p}\vec{p} \to \mathrm{jet(s)} + X$	$\vec{g}\vec{g} \to gg$ $\vec{q}\vec{g} \to qg$	Δg	(as above)
$\vec{p}\vec{p} \to \gamma + X$ $\vec{p}\vec{p} \to \gamma + \mathrm{jet} + X$ $\vec{p}\vec{p} \to \gamma\gamma + X$	$\vec{q}\vec{g} \to \gamma q$ $\vec{q}\vec{g} \to \gamma q$ $\vec{q}\vec{\bar{q}} \to \gamma\gamma$	Δg Δg $\Delta q, \Delta \bar{q}$	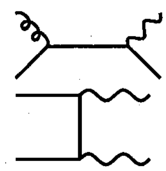
$\vec{p}\vec{p} \to DX,\ BX$	$\vec{g}\vec{g} \to c\bar{c},\ b\bar{b}$	Δg	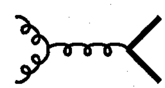
$\vec{p}\vec{p} \to \mu^+\mu^- X$ (Drell-Yan)	$\vec{q}\vec{\bar{q}} \to \gamma^* \to \mu^+\mu^-$	$\Delta q, \Delta \bar{q}$	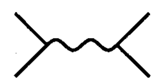
$\vec{p}\vec{p} \to (Z^0, W^\pm)X$ $p\vec{p} \to (Z^0, W^\pm)X$	$\vec{q}\vec{\bar{q}} \to Z^0,\ \vec{q}'\vec{\bar{q}} \to W^\pm$ $\vec{q}'\bar{q} \to W^\pm,\ q'\vec{\bar{q}} \to W^\pm$	$\Delta q, \Delta \bar{q}$	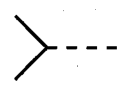

TABLE I. – *Key processes at RHIC for the determination of the parton distributions of the longitudinally polarized proton, along with the dominant contributing subprocesses, the parton distribution predominantly probed, and representative leading-order Feynman diagrams. From [8].*

relevant for RHIC-Spin, thanks to considerable efforts made over the past decade or so [28, 29, 30, 31, 32, 33]. These calculations bring the theoretical calculations for RHIC-Spin to the same level that has been so successful in the unpolarized case. For each of the processes in Table I the parton densities enter with different weights, so that each has its own role in helping to determine the polarized parton distributions. Some will allow a clean determination of gluon polarizations, others are more sensitive to quarks and antiquarks. Eventually, when data from RHIC will become available for most or all processes, a "global" analysis of the data, along with information from lepton scattering, will be performed which then determines the $\Delta q, \Delta\bar{q}, \Delta g$. For further details, see Sec. **3**˙5.

We will now discuss some of the recent results from RHIC on Δg, along with the associated theoretical predictions.

3·3. *Access to Δg in polarized proton-proton scattering at RHIC.* – The measurement of gluon polarization in the proton is a major focus and strength of RHIC [7, 8]. As we saw, several different processes will be investigated at RHIC [7, 8] that are very sensitive to gluon polarization: high-p_T prompt photons $pp \to \gamma X$, jet or hadron production $pp \to \text{jet}\, X$, $pp \to hX$, and heavy-flavor production $pp \to (Q\bar{Q})X$. An important role for the determination of Δg will also be played by measurements of two-particle, jet-jet (or hadron-hadron) and photon-jet correlations. For these, at the leading order approximation, the hard-scattering subprocess kinematics can be calculated directly on an event-by-event basis, giving an estimate of the gluon momentum fraction [34]. In addition, besides the current $\sqrt{s} = 200$ GeV, also $\sqrt{s} = 500$ GeV will be available at RHIC at a later stage. All this will allow to determine $\Delta g(x, Q^2)$ in various regions of x, and at different scales.

Results for $A_{\rm LL}$ in $pp \to \pi X$ are now available from PHENIX [35], and $A_{\rm LL}$ for single-inclusive jet production has been measured by STAR [36] (see also [9]). The results are shown in fig. 5. The curves shown in fig. 5 represent the $A_{\rm LL}$ values calculated at NLO for a range of gluon distributions from [37], from a suggested very large positive gluon polarization ("GRSV-max") with an integral $\Delta G = 1.9$ at scale $Q = 1$ GeV, to a "maximally" negative gluon polarization, ("$\Delta g = -g$"), for which $\Delta G(1\,{\rm GeV}^2) = -1.8$. The curves labeled "GRSV-std" represent the best fit of [37] to the polarized DIS data, which has a more "natural" $\Delta G(1\,{\rm GeV}^2)$ of about 0.4, and the results for "$\Delta g = 0$" correspond to very little gluon polarization, $\Delta G(1\,{\rm GeV}^2) = 0.1$.

One can see that the RHIC data are already discriminating between the various Δg distributions. For each of the channels studied so far, the results appear to rule out a very large gluon polarization, with either positive or (to a lesser extent) negative gluon polarization. The possibility that $\Delta G \gg 0$ was suggested [38] when the DIS experiments first discovered that the quarks (and anti-quarks) carry only very little of the proton spin. A large positive gluon polarization could mask a "bare" quark polarization [1]. At this point one cannot distinguish, however, between the gluon carrying 70% of the proton spin or carrying none of the proton spin, or determine the sign of the gluon polarization.

3·4. *Weak Boson Production.* – Within the standard model, W bosons are produced through pure $V - A$ interaction. Thus, in hadronic scattering, the helicity of the participating quark and antiquark are fixed in the reaction, making W production an ideal tool to study the spin structure of the nucleon [39].

To leading-order, Ws are produced through $u\bar{d} \to W^+$, for example. One can define a parity-violating single-longitudinal spin asymmetry as the difference of left-handed and right-handed production of Ws, divided by the sum:

$$A_L^W = \frac{d\sigma(-) - d\sigma(+)}{d\sigma(-) + d\sigma(+)} \,. \tag{18}$$

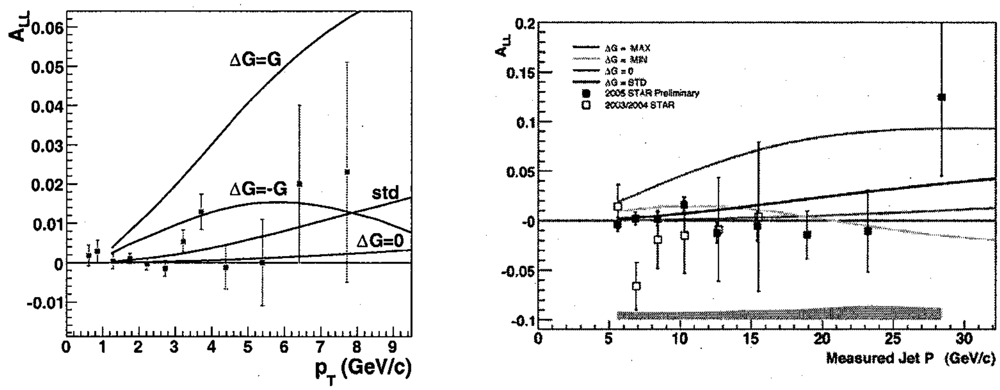

Fig. 5. – *Data for the double-spin asymmetry* A_{LL} *for mid-rapidity single-inclusive* π^0 *production at* $\sqrt{s} = 200$ *GeV from PHENIX (left, [35]) and for jet production from STAR (right, [36]).*

In the parton model, for the case of the process $u\bar{d} \to W^+$, one will have:

$$A_L^{W^+} = \frac{\Delta u(x_1)\bar{d}(x_2) - \Delta\bar{d}(x_1)u(x_2)}{u(x_1)\bar{d}(x_2) + \bar{d}(x_1)u(x_2)}. \tag{19}$$

To obtain the asymmetry for W^-, one interchanges u and d.

By identifying the rapidity of the W, y_W, relative to the *polarized* proton, we can obtain direct measures of the quark and antiquark polarizations, separated by quark flavor. The momentum fractions carried by the quarks and antiquarks, x_1 and x_2, can at LO be determined from y_W:

$$x_1 = \frac{M_W}{\sqrt{s}} e^{y_W}, \quad x_2 = \frac{M_W}{\sqrt{s}} e^{-y_W}. \tag{20}$$

From this one can easily see that $A_L^{W^+}$ approaches $\Delta u/u$ in the limit $y_W \gg 0$, whereas for $y_W \ll 0$ the asymmetry becomes $-\Delta\bar{d}/\bar{d}$. Expected sensitivities for measurements of $\Delta u/u$, $\Delta d/d$, $\Delta\bar{u}/\bar{u}$, $\Delta\bar{d}/\bar{d}$ at RHIC are shown in fig. 6. The experimental difficulty at RHIC is that the W is observed through its leptonic decay $W \to l\nu$, and only the charged lepton is observed. Since none of the detectors at RHIC is hermetic, measurement of missing transverse momentum is not available. It has been shown [40] that distributions in the rapidity of the charged lepton will also be powerful tools for measuring $\Delta u/u$, $\Delta d/d$, $\Delta\bar{u}/\bar{u}$, $\Delta\bar{d}/\bar{d}$.

3·5. *Global Analysis* . – The eventual determination of quark and gluon polarizations will require consideration of all existing data through a "global analysis" that makes simultaneous use of results for all probes, from RHIC and from lepton scattering. The technique is to optimize the agreement between measured spin asymmetries, relative to

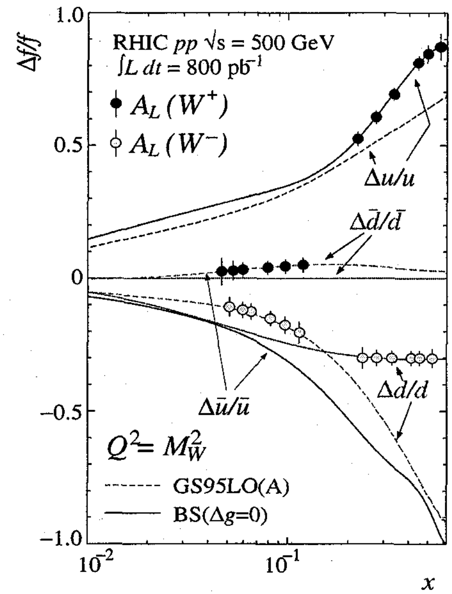

Fig. 6. – Expected sensitivity for the flavor-decomposed quark and antiquark polarization at RHIC. Darker points and error bars refer to the sensitivity from $A_L(W^+)$ measurements, and lighter ones correspond to $A_L(W^-)$.

the accuracy of the data, and the theoretical spin asymmetries, by minimizing the associated χ^2 function through variation of the shapes of the polarized parton distributions. The advantages of such a full-fledged global analysis program are manifold: (1) The information from the various reaction channels is all combined into a single result for $\Delta g(x), \Delta q(x), \Delta \bar{q}(x)$. (2) The global analysis effectively deconvolutes the experimental information, which in its raw form is smeared over the fractional gluon momentum x, and fixes the gluon distribution at definite values of x. Figure 7 highlights the importance of this. The figure shows [41] the contributions of the various regions in gluon momentum fraction to the mid-rapidity spin-dependent cross section for $pp \to \pi^0 X$ at RHIC, for six different sets of polarized parton distributions [37] mostly differing in the gluon distribution. The pion's transverse momentum was chosen to be 2.5 GeV. One can see that the distributions are very broad, and that the x-region that is mostly probed depends itself on the size and form of the polarized gluon distribution. This makes it very difficult to assign a good estimate of the gluon momentum fraction to a data point at a given pion transverse momentum. The global analysis solves this problem.

The further advantages of a global analysis are: (3) State-of-the-art (NLO) theoretical calculations can be used without approximations. (4) It provides a framework to determine errors on the quark and gluon polarizations. (5) Correlations with other experiments, to be included in χ^2 and sensitive to degrees of freedom different from Δg, are automatically respected. Global analyses of this type have been developed very success-

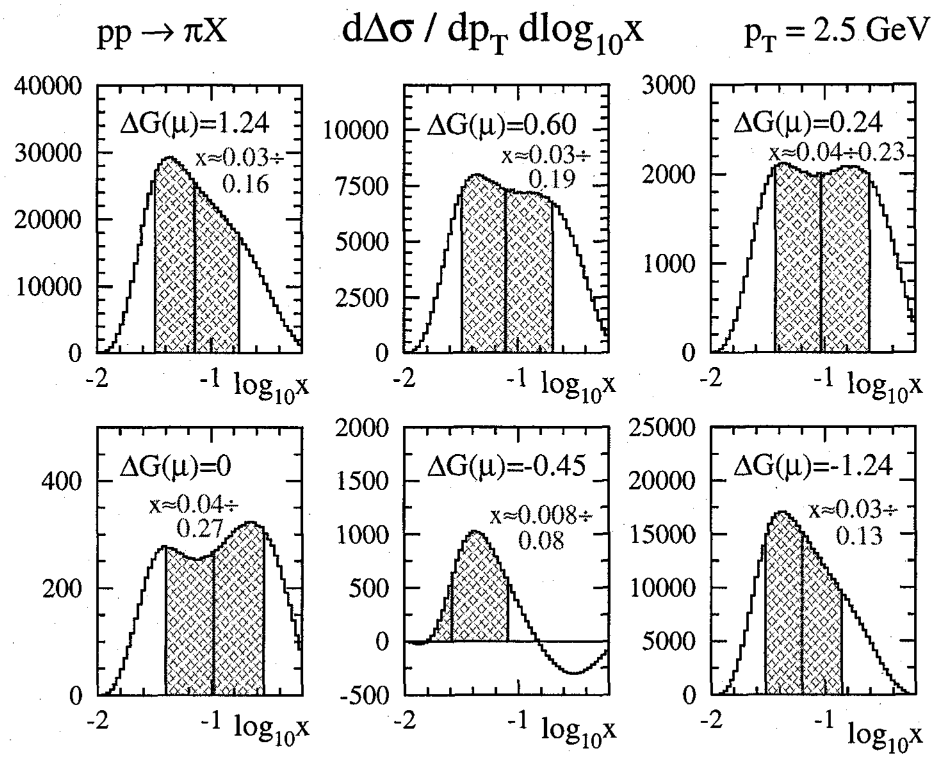

Fig. 7. – NLO $d\Delta\sigma/dp_T d\log_{10}(x)$ (arbitrary normalization) for the reaction $pp \to \pi^0 X$ at RHIC, for $p_T = 2.5\,\mathrm{GeV}$ and six different values for $\Delta G(\mu^2)$ at $\mu \approx 0.4$ GeV [37]. The shaded areas denote in each case the x-range dominantly contributing to $d\Delta\sigma$. From [41].

fully over many years for unpolarized parton densities. Examples of early work on global analyses of RHIC-Spin and polarized DIS data in terms of polarized parton distributions are [42, 43, 44].

4. – Collisions of transversely polarized protons

4·1. *Transversity*. – Besides the unpolarized and the helicity-dependent densities, there is a third set of leading-twist parton distributions, transversity [45]. They measure the net number (parallel minus antiparallel) of partons with transverse polarization in a transversely polarized nucleon:

$$\delta f(x, Q^2) = f^{\uparrow}(x, Q^2) - f^{\downarrow}(x, Q^2)\,. \tag{21}$$

In a helicity basis, one finds that transversity corresponds to a helicity-flip structure, which precludes a gluon transversity distribution at leading twist [46]. It also makes transversity a probe of chiral symmetry breaking in QCD [47]: perturbative-QCD interactions preserve chirality, and so the helicity-flip required to make transversity non-zero must primarily come from soft non-perturbative interactions for which chiral symmetry is broken.

In contrast to the distributions f and Δf, we have essentially no knowledge from experiment so far about the transversity distributions δf. Again the fact that perturbative interactions in the Standard Model do not change chirality means that inclusive DIS is not useful. Collins, however, showed [47] that properties of fragmentation might be exploited to obtain a "transversity polarimeter": a pion produced in fragmentation will have some transverse momentum $\vec{k}_T$ with respect to the momentum of the transversely polarized fragmenting parent quark. There may then be a correlation of the form $\vec{S}_T \cdot (\vec{P}_\pi \times \vec{k}_\perp)$. The fragmentation function associated with this correlation is the Collins function. It makes a leading-power [47] contribution to the single-spin asymmetry $A_\perp$ in the reaction $ep^\uparrow \to e\pi X$:

$$A_\perp \propto |\vec{S}_T| \sin(\phi + \phi_S) \sum_q e_q^2 \delta q(x) H_1^{\perp,q}(z) \, , \tag{22}$$

where ϕ (ϕ_S) is the angle between the lepton plane and the $\gamma^*\pi$-plane (and the transverse target spin). HERMES has reported clear signs of a nonvanishing Collins asymmetry in $ep^\uparrow$ scattering [13]. Recently, first independent information on the Collins functions has come from BELLE measurements in e^+e^- annihilation [48]. This has allowed to obtain a first "glimpse" of transversity from a combined analysis of single-transverse spin asymmetries in semi-inclusive deep-inelastic scattering (SIDIS) and the BELLE data [49].

Clean and direct information on transversity might be gathered from polarized proton-proton collisions at RHIC, using the Drell-Yan process [7, 8]. In pp collisions, however, the Drell-Yan process probes products of valence quark and sea antiquark distributions. It is possible that antiquarks in the nucleon carry only little transverse polarization since the perturbative generation of transversity sea quarks from $g \to q\bar{q}$ splitting is missing. Also, at RHIC the partonic momentum fractions are fairly small, so that the denominator of A_{TT} is large. NLO studies [50] estimate the size of A_{TT} at RHIC to be at most a few per cent.

It has recently been proposed to add polarization to planned $\bar{p}p$ experiments at the GSI-FAIR facility, and to extract transversity from measurements of A_{TT} for the Drell-Yan process [51, 52]. Initially, experiments could be performed in a fixed-target mode, using the 15 GeV antiproton beam. At later stages of operations, there are plans for an asymmetric $\bar{p}p$ collider, with an additional proton beam of energy 3.5 GeV. The results from such measurements would be complementary to what can be obtained from RHIC or SIDIS. In $\bar{p}p$ collisions the Drell-Yan process mainly probes products of two *quark* densities, $\delta q \times \delta q$, since the distribution of antiquarks in antiprotons equals that of quarks in the proton. In addition, kinematics in the proposed experiments are such that

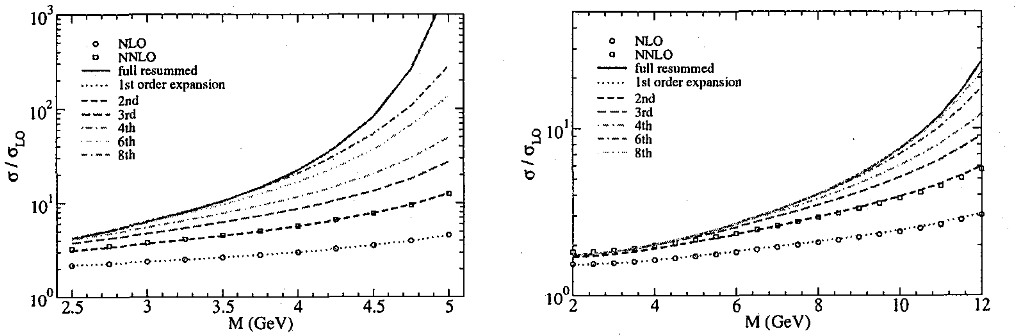

Fig. 8. – "K-factors" for the Drell-Yan cross section in fixed-target $\bar{p}p$ collisions at $s = 30$ GeV^2 (left) and for an asymmetric collider mode with $s = 210$ GeV^2 (right), as functions of lepton pair invariant mass M. For details, see [55].

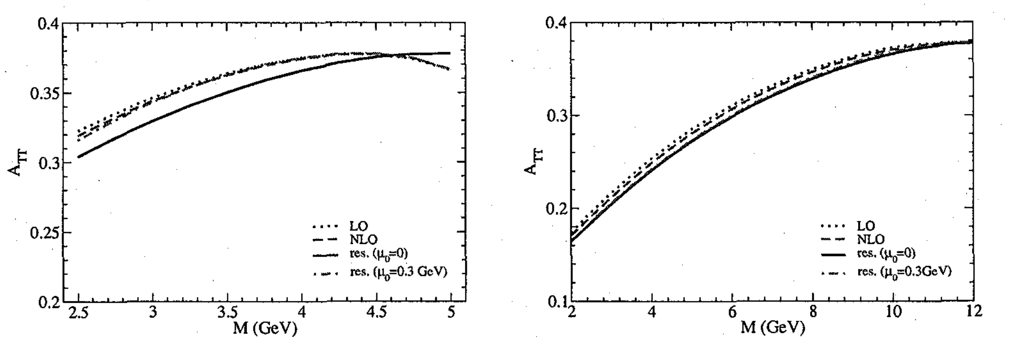

Fig. 9. – Corresponding spin asymmetries $A_{\rm TT}(\phi = 0)$ at LO, NLO and for the NLL resummed case.

rather large partonic momentum fractions, $x \sim 0.5$, are probed. One therefore accesses the valence region of the nucleon, where the polarization of partons is expected to be large. Estimates [52] for the GSI PAX and ASSIA experiments show that the expected spin asymmetry $A_{\rm TT}$ should indeed be very large, of order 30% or more.

The theoretical framework for GSI kinematics is somewhat more involved than for RHIC, since in the region to be accessed higher-order corrections to the partonic cross sections are particularly important. The NLO corrections for the transversely polarized Drell-Yan cross section have been calculated in [53]. In the region of interest here, however, certain logarithmic terms in the partonic cross section become important to *all* orders in perturbation theory and need to be resummed. Such a "threshold resummation" is a well established technique in QCD [54]. For $A_{\rm TT}$ for the Drell-Yan process it has been addressed in detail recently in [55].

Figure 8 shows results of [55] for the K $(= \sigma^{\text{higher-order}}/\sigma^{LO})$ factors for the unpolarized Drell-Yan cross section at $s = 30\ \mathrm{GeV}^2$ (left) and $s = 210\ \mathrm{GeV}^2$ (right), at NLO, NNLO, and for the next-to-leading logarithmic (NLL) resummed case, along with various higher-order expansions of the resummed result. As can be seen, the corrections are very large, in particular in the lower-energy case. Figure 9 shows the corresponding spin asymmetries A_{TT}. A_{TT} turns out to be extremely robust and remarkably insensitive to higher-order corrections. Perturbative corrections thus make the cross sections larger independently of spin. They would therefore make easier the study of spin asymmetries, and ultimately transversity distributions. For further details, including a discussion on the role of nonperturbative effects, see [55]. We finally note that it has recently also been proposed [56] to study the spin asymmetry A_{TT} for the reaction $\bar{p}p \to \pi^0 X$, which would give additional information on transversity.

4·2. *Single-transverse spin asymmetries.* – As we mentioned in the introduction, there have been observations of striking single-transverse-spin effects in hadronic scattering. Large single-spin asymmetries in single-inclusive pion production persist to RHIC energies, as seen by STAR [57] and BRAHMS [58]. At PHENIX [59], the asymmetry was studied in the mid-rapidity regime, where it was found to be small.

The observed large size of SSAs in hadronic scattering has presented a challenge for QCD theorists [45, 60]. Two mechanisms have been discussed [61, 62, 63, 64] and extensively applied [63, 65, 66, 67] in phenomenological studies. The first relies on the use of transverse-momentum dependent parton distributions for the transversely polarized proton. For these distributions, known as Sivers functions [61], the parton transverse momentum is assumed to be correlated with the proton spin vector, so that spin asymmetries naturally arise from the directional preference expressed by that correlation. The other mechanism (referred to as Efremov-Teryaev-Qiu-Sterman (ETQS) mechanism) is formulated in terms of the collinear factorization approach and twist-three transverse-spin-dependent quark-gluon correlation functions of the proton [62, 63, 64].

A concept common to both mechanisms is the factorization of the spin-dependent cross section into functions describing the distributions of quarks and gluons in the polarized proton, and partonic hard-scattering cross sections, calculated in QCD perturbation theory. The question of which mechanism should be used in the analysis of a single-spin asymmetry is therefore primarily tied to the factorization theorem that applies for the single-spin observable under consideration. For the single-inclusive process $p^\uparrow p \to \pi X$, there is only one hard scale, the transverse momentum $\ell_\perp$ of the produced pion, and the SSA is power-suppressed ("higher-twist") by $1/\ell_\perp$. In this case, one can prove a *collinear* factorization theorem in terms of the quark-gluon correlation functions [63, 64], and the ETQS mechanism applies. On the other hand, the observables typically investigated in deep-inelastic lepton scattering are characterized by a large scale Q (the virtuality of the DIS photon) and by the much smaller, and also measured, transverse momentum $q_\perp$ of the produced hadron. In this two-scale case, single-spin asymmetries may arise at leading twist, i.e., *not* suppressed by $1/Q$. The relevant factorization theorem is formulated in terms of *transverse-momentum-dependent* (TMD) functions [68, 69, 70, 71], in particular the Sivers functions.

In the following, we will describe both types of observables, the single-spin asymmetry in single-inclusive scattering and the asymmetry in a "two-scale" situation. We will also discuss recent work [72] that has connected the two mechanisms in the case of the single-spin asymmetry for the Drell-Yan process.

4·3. *Single transverse-spin asymmetry in high-$\ell_\perp$ pion production in pp collisions* . – The single-transverse spin asymmetry in the process $pp \to \pi X$ is among the simplest spin observables in hadronic scattering. One scatters a beam of transversely polarized protons off unpolarized protons and measures the numbers of pions produced to either the left or the right of the plane spanned by the momentum and spin directions of the initial polarized protons. This defines a "left-right" asymmetry. Equivalently, the asymmetry may be obtained by flipping the spins of the initial polarized protons. This gives rise to the customary definition

$$A_N(\ell, \vec{s}_T) \equiv \frac{\sigma(\ell, \vec{s}_T) - \sigma(\ell, -\vec{s}_T)}{\sigma(\ell, \vec{s}_T) + \sigma(\ell, -\vec{s}_T)} \equiv \frac{\Delta\sigma(\ell, \vec{s}_T)}{\sigma(\ell)} , \tag{23}$$

where $\vec{s}_T$ denotes the transverse spin vector and ℓ the four-momentum of the produced pion. We assume the pions to be produced at large transverse momentum $\ell_\perp$.

As we mentioned above, measurements of single-spin asymmetries in hadronic scattering experiments over the past three decades have shown spectacular results. Large asymmetries of up to several tens of per cents were observed at forward (with respect to the polarized initial beam) angles of the produced pion. Until a few years ago, all these experiments were done with a polarized beam impeding on a fixed target [12]. These experiments necessarily had a relatively limited kinematic reach, in particular in $\ell_\perp$. Now, with RHIC, it has become possible to investigate A_N at higher energies [57, 58, 59], in a kinematic regime where the theoretical description is bound to be under better control. Indeed, as we saw in Figure 2, at RHIC also the unpolarized pion production cross section has been measured, in the same kinematic regimes as covered by the measurements of the single-spin asymmetries, and is well described by the NLO perturbative calculations based on collinear factorization.

Despite the conceptual simplicity of A_N, the theoretical analysis of single-spin asymmetries in hadronic scattering is remarkably complex. The reason for this is that the asymmetry for a single-inclusive reaction like $p^\uparrow p \to \pi X$ (the symbol $\uparrow$ denoting from now on the polarization of the proton) is power-suppressed as $1/\ell_\perp$ in the hard scale set by the observed large pion transverse momentum. This is in contrast to typical double (longitudinal or transverse) spin asymmetries that usually scale for large $\ell_\perp$. In essence, the leading-twist part cancels in the difference $\sigma(\ell, \vec{s}_T) - \sigma(\ell, -\vec{s}_T)$ in the numerator of A_N. That A_N must be power-suppressed is easy to see: the only leading-power distribution function in the proton associated with transverse polarization is *transversity.* For transversity to contribute, the corresponding partonic hard-scattering functions need to involve a transversely polarized quark scattering off an unpolarized one. Cross sections for such reactions vanish in perturbative QCD for massless quarks because they require a helicity-flip for the polarized quark, which the perturbative $q\bar{q}g$ vertex does not allow.

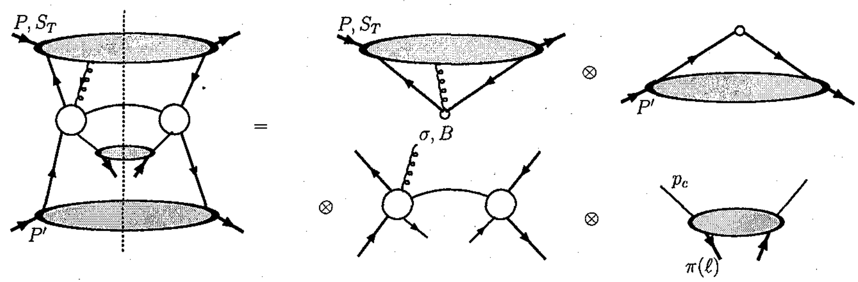

Fig. 10. – Generic Feynman diagram contributing to the single transverse-spin asymmetry for inclusive pion production in proton-proton scattering at leading twist (twist-three). The polarized cross section can be factorized into convolutions of the following terms: twist-three quark-gluon correlation functions for the transversely polarized proton, parton distributions for the unpolarized proton, pion fragmentation functions, and hard-scattering functions calculable in QCD perturbation theory.

In addition, a non-vanishing single-spin asymmetry requires the presence of a relative interaction phase between the interfering amplitudes for the different helicities. At leading twist this phase can only arise through a loop correction, which is of higher-order in the strong coupling constant and hence leads to a further suppression. These arguments are, in fact, more than 30 years old [73] and led to the general expectation that single-spin asymmetries should be very small, in striking contrast with the experimental results.

Power-suppressed contributions to hard-scattering processes are generally much harder to describe in QCD than leading-twist ones. In the case of the single-spin asymmetry in $pp \to \pi X$, a complete and consistent framework could be developed, however [63]. It is based on a collinear factorization theorem at non-leading twist that relates the single-spin cross section to convolutions of twist-three quark-gluon correlation functions for the polarized proton with the usual parton distributions for the unpolarized proton and the pion fragmentation functions, and with hard-scattering functions calculated from an interference of two partonic scattering amplitudes: one with a two-parton initial state and the other with a three-parton initial state [62, 63]. A generic Feynman diagram for the scattering process is shown in Figure 10, along with its factorization just described. Typical Feynman diagrams for the hard-scattering in case of quark-gluon scattering are shown in Figure 11. As was shown in [63], the phase needed to generate a single-spin asymmetry arises naturally in the hard-scattering functions, even at tree level, thanks to its pole structure. Imaginary parts arise from the scattering amplitude with an extra initial-state gluon when its momentum integral is evaluated by the residues of unpinched poles of the propagators indicated by the bars in Figure 11. The on-shell condition associated with any such pole fixes the momentum fraction of the extra initial-state gluon. Roughly speaking, all of the diagrams in Figure 11 provide an unpinched pole at $x_1 = x_2$ [63]. After a collinear expansion, one finds the following expression for the spin-dependent cross section:

$$E_\ell \frac{d^3\Delta\sigma(\vec{s}_T)}{d^3\ell} \propto \sum_{a,b,c} D_{c\to h}(z) \otimes f_b(x') \otimes \left[T_{a,F}(x,x) - x\left(\frac{d}{dx}T_{a,F}(x,x)\right)\right] \otimes H_{ab\to c}(\hat{s},\hat{t},\hat{u}) \,, \tag{24}$$

where $\hat{s}, \hat{t}, \hat{u}$ are the partonic Mandelstam variables, $f_b(x')$ and $D_{c\to h}(z)$ are the usual unpolarized parton distribution and fragmentation functions, respectively, and the twist-three functions $T_{a,F}$ are defined as

$$T_{a,F}(x_1,x_2) = \int \frac{dy_1^- dy_2^-}{4\pi} e^{ix_1P^+y_1^- + i(x_2-x_1)P^+y_2^-} \times \langle P, \vec{s}_T | \bar{\psi}_a(0)\gamma^+ \left[\epsilon^{s_T\sigma n\bar{n}}\, F_\sigma{}^+(y_2^-)\right] \psi_a(y_1^-) | P, \vec{s}_T\rangle \,. \tag{25}$$

The sum in eq. (25) runs over all flavors, with $H_{ab\to c}$ the associated hard-scattering functions, calculated from diagrams like the ones shown in Figure 11. The $H_{ab\to c}$ are power-suppressed with respect to their unpolarized counterparts, and they are also down by $\sqrt{\alpha_s}$ due to the additional gluon that couples in the diagrams. As one can see, a specific combination of the $T_{a,F}$ occurs in eq. (25), involving the derivative of $T_{a,F}$. Such derivative terms arise in the collinear expansion, because there are terms proportional to the initial partons' transverse momenta in the δ-functions fixing the light-cone momentum fractions [63]. The other terms in eq. (25) that involve $T_{a,F}(x,x)$ without a derivative, were recently derived in [67].

Based on eq. (25), one can perform some phenomenology for the single-spin asymmetry, examining the salient features of the new RHIC data and of the earlier E704 fixed-target pion production data. In [67] a simple model ansatz for the twist-three quark-gluon correlation functions $T_{a,F}(x,x)$ ($a = u, \bar{u}, d, \bar{d}, s, \bar{s}$) was made, relating them to their unpolarized leading-twist counterparts:

$$T_{a,F}(x,x) = N_a\, x^{\alpha_a}\, (1-x)^{\beta_a}\, f_a(x) \,, \tag{26}$$

The parameters in this ansatz were determined through a "global" fit to the experimental data for A_N as functions of Feynman-x_F. As one example, fig. 12 compares the fit results to the experimental data from RHIC. The overall quality of the fit is relatively poor, but the basic trends of the data are reproduced. With new precise experimental information expected to arrive from RHIC, however, we will be entering an era where detailed global analyses of the data on A_N will become possible.

4·4. *Single transverse-spin asymmetries in two-scale situations.* – As we discussed earlier, further exciting single-spin phenomena may occur when one has observables characterized by two very separate momentum scales, a hard scale Q, and a much lower measured transverse momentum $q_\perp$. For such observables one may have a factorization

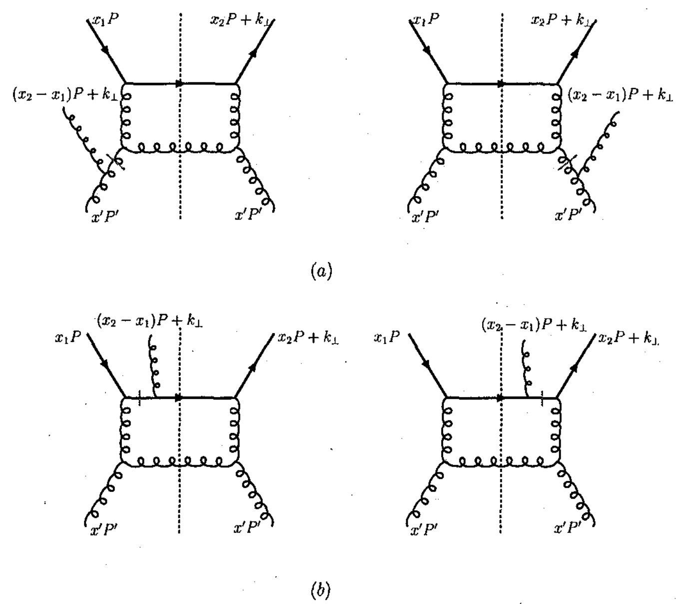

Fig. 11. – Specific examples of twist-three diagrams for generic (a) initial-state and (b) final-state interactions.

in terms of transverse-momentum-dependent (TMD) functions. Among these are the Sivers functions [61], which are TMD parton distributions. They represent distributions of unpolarized quarks of flavor a in a transversely polarized nucleon, through a correlation between the quark's transverse momentum $\vec{k}_\perp$ and the nucleon polarization vector $\vec{s}_T$:

$$\hat{f}_a(x, \boldsymbol{k}_\perp, \boldsymbol{s}_T) = f_a(x, k_\perp) + \frac{1}{2}\Delta^N f_a(x, k_\perp)\frac{\boldsymbol{s}_T \cdot (\boldsymbol{P} \times \boldsymbol{k}_\perp)}{|\boldsymbol{s}_T|\,|\boldsymbol{P}|\,|\boldsymbol{k}_\perp|}\,, \tag{27}$$

where the function $f_a(x, k_\perp)$ with $k_\perp = |\boldsymbol{k}_\perp|$ is the unpolarized TMD parton distribution, and $\Delta^N f_a$ denotes the Sivers function. The latter is also sometimes written as

$$\Delta^N f_a(x, k_\perp) \equiv -\frac{2k_\perp}{M_N}\, f_{1T}^{\perp a}(x, k_\perp)\,. \tag{28}$$

For the Sivers function to exist, final/initial-state interactions are required, as well as an interference between different helicity Fock states of the nucleon. In the absence of interactions, the Sivers function would vanish by time-reversal invariance of QCD, hence it is often referred to as a "naively time-reversal-odd" distribution. As was shown in [74, 75, 76], the interactions are represented in a natural way by the gauge link that is required for a gauge-invariant definition of a TMD parton distribution. Interference

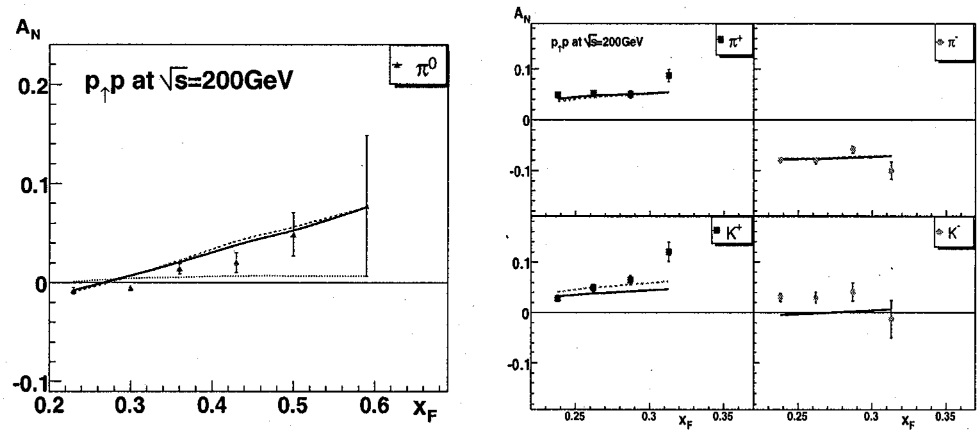

Fig. 12. – Comparison of the single-spin asymmetries A_N using the fit results of [67] to the RHIC data by the STAR [57] (left) and BRAHMS [58] (right) collaborations. The lower dotted line in the figure shows the contribution to A_N by the "non-derivative" terms alone.

between different helicity Fock states implies the presence of orbital angular momentum [74, 77]. The Sivers functions have also been linked to spatial distributions of partons in the proton [77, 78, 79, 80]. These properties motivate the study of this function.

The Sivers function will contribute to the target SSA in semi-inclusive DIS, but also to SSAs in polarized pp scattering processes such as the Drell-Yan process and di-jet or jet-photon correlations. A particularly interesting aspect is that the Sivers functions are not universal in the usual sense, i.e., they are not the same in each hard-scattering process. This might at first sight appear to make the study of these functions less interesting. However, the non-universality has in fact a clear physical origin, and its closer investigation has turned out to be an extremely important and productive development in QCD. We will only describe it qualitatively here. We have already mentioned that, in order to be non-zero, the Sivers functions require an additional final/initial-state interaction, represented by the gauge-link that makes the function gauge-invariant. This may be viewed as a rescattering of the parton in the color field of the nucleon remnant. Depending on the process, the associated color Lorentz forces will act in different ways on the parton. In DIS, so far explored experimentally, the final-state interaction between the struck parton and the nucleon remnant is attractive. In contrast, for the Drell-Yan process it is repulsive. Therefore, the Sivers functions contribute with opposite signs to the single-spin asymmetries for these two processes [74, 75, 76]. This is a remarkable and fundamental prediction that really tests all concepts we know of for analyzing hard-scattering reactions in strong interactions. The verification of the predicted non-universality of the Sivers functions is an outstanding challenge in strong-interaction physics.

Let us give a simple QED example [81] that captures the essential physics. In fig. 13(a) we consider a "toy" DIS process. A transversely polarized charge-less "hadron", consist-

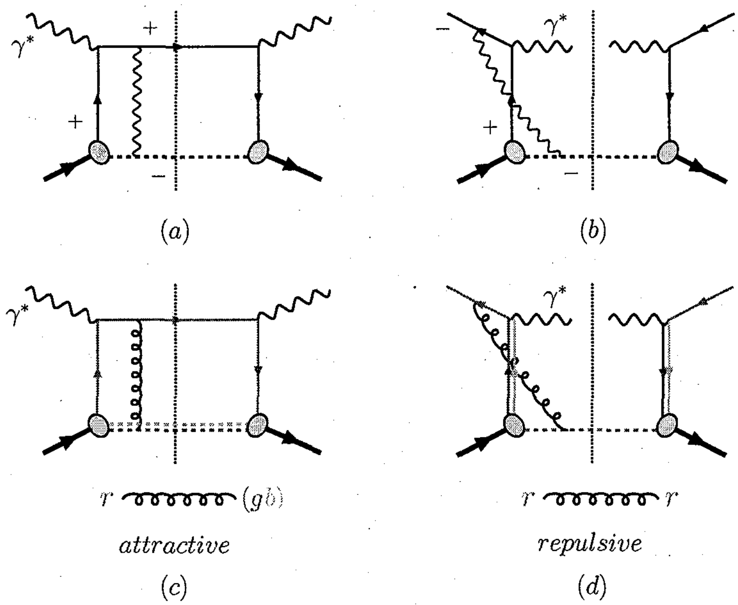

Fig. 13. – *(a),(b) Simple QED example for process-dependence of the Sivers functions in DIS and the Drell-Yan process. (c),(d) Same for QCD.*

ing of particles with electric charges $+1$ and -1, is probed by a highly virtual photon. In order not to be forced to vanish by time-reversal invariance, a single-spin asymmetry for the process requires the presence of an interaction phase. Such a phase may be generated by a rescattering of the struck "parton" in the field of the "hadron remnant", by exchange of a photon as shown in the figure. The amplitude with the additional exchanged photon interferes with that without the photon. More precisely, two different phases appear, the S and P-wave Coulomb phases. The difference of these phases is infrared-finite and generates the single-spin asymmetry [74]. As the electric charges of the two interacting particles are opposite, this final-state interaction is *attractive.*

Now consider a similar model for the Drell-Yan process in fig. 13(b). "Partons" of opposite charge annihilate to produce a highly virtual photon. The interaction generating the phase in this case is "initial-state" and is between the remnant of the transversely polarized "hadron" and the initial parton from the other, unpolarized, "hadron". These necessarily have identical charges, and the interaction is *repulsive.* As a result, the spin-effect in this case needs to be of opposite sign as that in DIS.

These simple models are readily generalized to true hadronic scattering in QCD. In DIS, the final-state interaction is through a gluon exchanged between the $\mathbf{3}$ and $\bar{\mathbf{3}}$ states of the struck quark and the nucleon remnant, which is attractive, as indicated in fig. 13(c). In the Drell-Yan process, the interaction is between the $\mathbf{3}$ and $\mathbf{3}$ states (or $\bar{\mathbf{3}}$ and $\bar{\mathbf{3}}$) and therefore repulsive, as shown in fig. 13(d). This is the essence of the – by now widely quoted – result that the Sivers functions contributing to DIS and to the Drell-Yan process

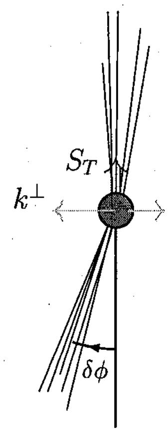

Fig. 14. – "Asymmetric jet correlation". The proton beams run perpendicular to the drawing.

have opposite sign [74, 75, 76, 82]:

$$f_{1T}^{\perp a}(x, k_{\perp})\Big|_{\mathrm{DY}} = -f_{1T}^{\perp a}(x, k_{\perp})\Big|_{\mathrm{DIS}} . \tag{29}$$

In the full gauge theory, the phases generated by the additional (final-state or initial-state) interactions can be summed to all orders into a "gauge-link", which is a path-ordered exponential of the gluon field and makes the Sivers functions gauge-invariant. The non-universality of the Sivers functions is then reflected in a process-dependence of the space-time direction of the gauge-link. The crucial role played by the gauge link has given rise to intuitive model interpretations of single-spin asymmetries in terms of spatial deformations of parton distributions in a transversely polarized nucleon [79].

The process-dependence of the Sivers functions can also be tested in more complicated QCD hard-scattering. An example is the single-spin asymmetry in di-jet angular correlations [83, 84]. The basic idea is very simple and presented in Figure 14. As we discussed above, the Sivers function represents a correlation of the form $\boldsymbol{s}_T \cdot (\boldsymbol{P} \times \boldsymbol{k}_{\perp})$ between the transverse proton polarization vector, its momentum, and the transverse momentum of the parton relative to the proton direction. In other words, if there is a Sivers-type correlation then there will be a preference for partons to have a component of intrinsic transverse momentum to one side, perpendicular to both $\boldsymbol{s}_T$ and $\boldsymbol{P}$. Suppose now for simplicity that one observes a jet in the direction of the proton polarization vector, as shown in Figure 14. A "left-right" imbalance in $\boldsymbol{k}_{\perp}$ of the parton will then affect the $\Delta\phi$ distribution of jets nearly opposite to the first jet and give the cross section an asymmetric piece around $\Delta\phi = \pi$.

Tremendous progress has been made recently in our understanding of the gauge links for this observable [85]. The more involved color structure of the hard-scattering functions has profound consequences on the gauge links. It was found that if all interactions are summed up, the resulting gauge link for the TMD parton distributions takes a much more complicated form. It does not involve just the color charge of the relevant parton, but has in general knowledge about the full hard-scattering process and its color structure. As such, different correlators were found to appear in different partonic channels, even if the parton type entering from the polarized proton is the same. This observation makes the non-universality of the TMD parton distributions much more dramatic than previously indicated by their sign difference between the SIDIS and Drell-Yan processes. Ref. [86] stressed that the non-trivial gauge link structure found in [85] implies that a "standard" factorization in terms of universal TMD parton distributions cannot hold for this process. Standard factorization still holds to first order in perturbation theory [87] but breaks down beyond [88]. The STAR collaboration has now published first experimental data for the single-spin asymmetry in di-jet correlations [89], which show an asymmetry consistent with zero. Clearly, the field is moving ahead at a remarkable pace!

4·5. *Relation between mechanisms for single-spin asymmetries.* – From what we discussed so far, the two mechanisms for single-spin asymmetries, twist-three quark-gluon correlation functions on the one hand and TMD distributions on the other, might appear to be essentially unrelated. However, one can make an argument that a consistent theoretical description of the SSA for a hard process over its full kinematical regime requires both mechanisms to be present and to contain the same physics in the region where they both apply. To give a specific example, let us consider the SSA for the Drell-Yan process when the invariant mass Q of the pair as well as its transverse momentum $q_\perp$ are measured [72].

At relatively large pair transverse momentum, $q_\perp \sim Q$, there is only one large scale, and the SSA will be power-suppressed in that scale. This directs us to use the ETQS mechanism with its collinear factorization involving the twist-three quark-gluon correlation functions and corresponding hard-scattering functions calculated at lowest order from partonic $3 \to 2$ processes, as described in subsection 4·3.

We can next investigate what happens in this case when we make the ratio $q_\perp/Q$ small, keeping however both scales perturbative, $Q \gg q_\perp \gg \Lambda_{\rm QCD}$. We refer to $q_\perp$ in this regime as "moderate" transverse momentum. The ETQS mechanism will still apply here (even though the hard-scattering functions will develop large logarithms of the ratio $q_\perp/Q$ that will eventually need to be resummed to all orders in the strong coupling). At the same time, however, the factorization in terms of TMD distributions applies now [68, 69, 70], which involves the Sivers functions. If both mechanisms are internally consistent, they must describe the same physics in this region.

In recent publications [72], it was demonstrated that the two mechanisms indeed provide the same description of the single-spin asymmetry for the Drell-Yan process in the regime $\Lambda_{\rm QCD} \ll q_\perp \ll Q$, and that there is a direct correspondence between the Sivers functions and the twist-three quark-gluon correlation functions. The key observation is that, at moderate transverse momentum, the Sivers function may be calculated perturbatively, using the twist-three quark-gluon correlation functions. In other words, the ETQS mechanism generates a non-vanishing Sivers function in this kinematic regime.

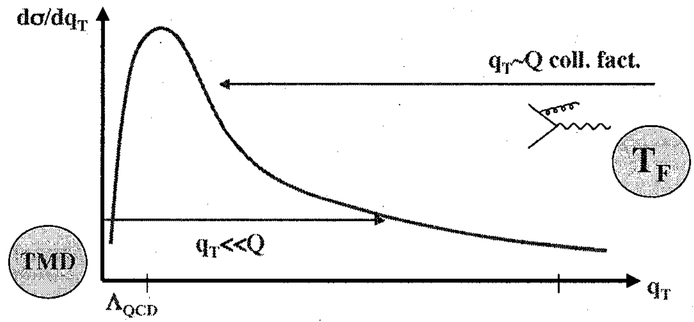

Fig. 15. – Cartoon of different kinematic regions $q_\perp \sim Q$ and $q_\perp \gg \Lambda_{\rm QCD}$ relevant for the single-spin asymmetry in the Drell-Yan process. In the region of overlap, $Q \gg q_\perp \gg \Lambda_{\rm QCD}$ both mechanisms describe the same physics [72].

These results may in some sense be viewed as establishing a unification of the two mechanisms. At large $q_\perp$, the ETQS mechanism applies. At moderate transverse momentum, a smooth transition from the ETQS mechanism to the one based on TMD factorization occurs, with the two approaches containing the same physics. At yet lower $q_\perp$ ($\sim \Lambda_{\rm QCD}$), the TMD factorization still applies, containing in a natural way the transition from perturbative to non-perturbative physics. A cartoon of this connection between the two mechanisms is given in Figure 15. This unified picture should prove to be the best approach to phenomenological studies of single-spin asymmetries.

* * *

I thank Mauro Anselmino for the kind invitation to the International School of Physics Enrico Fermi "Strangeness and Spin in Fundamental Physics". I am grateful to M. Stratmann and F. Yuan for useful discussions. I am also grateful to the U.S. Department of Energy (contract number DE-AC02-98CH10886) for providing the facilities essential for the completion of his work.

REFERENCES

[1] Leader E., *these proceedings. For reviews, see:* Hughes E.W. and Voss R., *Ann. Rev. Nucl. Part. Sci.* **49** (1999) 303; Filippone B.W. and Ji X.D., *Adv. Nucl. Phys.* **26** (2001) 1; Bass S.D., *Rev. Mod. Phys.* **77** (2005) 1257.
[2] Jaffe R.L. and Manohar A., *Nucl. Phys.* **B337** (1990) 509; Ji X.D., *Phys. Rev. Lett.* **78** (1997) 610; Bakker B.L.G., Leader E., Trueman T.L., *Phys. Rev.* **D70** (2004) 114001; Ji X.D., Tang J., Hoodbhoy P., *Phys. Rev. Lett.* **76** (1996) 740.

[3] Hoodbhoy P., Ji X.D., Lu W., *Phys. Rev.* **D59** (1999) 074010.
[4] Jaffe R.L., *these proceedings.*
[5] Ageev E.S. *et al.* [COMPASS Collaboration], *Phys. Lett.* **B633** (2006) 25.
[6] Airapetian A. *et al.* [HERMES Collaboration], *Phys. Rev. Lett.* **84** (2000) 2584; Liebing P., AIP Conf.Proc. 915 (2007) 331.
[7] Bunce G., Saito N., Soffer J., Vogelsang W., *Annu. Rev. Nucl. Part. Sci.* **50** (2000) 525.
[8] Aidala C. *et al.*, `http://spin.riken.bnl.gov/rsc/report/masterspin.pdf` *(Research Plan for Spin Physics at RHIC)*; *update:* Bunce G. *et al.*, `http://www.physics.rutgers.edu/np/RHIC_spin_LRP07.pdf`
[9] Saito N., *these proceedings.*
[10] Anselmino M., *these proceedings.*
[11] Hasch D., *these proceedings.*
[12] Adams D.L. *et al.* [E581 and E704 Collaborations], *Phys. Lett.* **B261** (1991) 201; Adams D.L. *et al.* [FNAL-E704 Collaboration], *Phys. Lett.* **B264** (1991) 462; Krueger K. *et al.*, *Phys. Lett.* **B459** (1999) 412.
[13] Bravar A. [Spin Muon Collaboration], *Nucl. Phys.* **A666** (2000) 314; Airapetian A. *et al.* [HERMES Collaboration], *Phys. Rev. Lett.* **84** (2000) 4047; *Phys. Rev.* **D64** (2001) 097101; *Phys. Rev. Lett.* **94** (2005) 012002; Diefenthaler M. [HERMES Collaboration], AIP Conf.Proc. **792** (2005) 933; arXiv:0706.2242 [hep-ex]; Avakian H. [CLAS Collaboration], *these proceedings*; Alexakhin V.Y. *et al.* [COMPASS Collaboration], *Phys. Rev. Lett.* **94** (2005) 202002.
[14] Gross D.J. and Wilczek F., Phys. Rev. Lett. **30** (1973) 1343; Politzer H.D., *ibid.* 1346.
[15] Sterman G. and Weinberg S., Phys. Rev. Lett. **39** (1977) 1436.
[16] Dokshitzer Y.L., *Sov. Phys. JETP* **46** (1977) 641; Lipatov L.N., *Sov. J. Nucl. Phys.* **20** (1975) 95; Gribov V.N. and Lipatov L.N., *Sov. J. Nucl. Phys.* **15** (1972) 438.
[17] Altarelli G. and Parisi G., *Nucl. Phys.* **B126** (1977) 298.
[18] Ahmed M.A. and Ross G.G., *Nucl. Phys.* **B111** (1976) 441.
[19] Mertig R. and van Neerven W., *Z. Phys.* **C70** (1996) 637; Vogelsang W., *Phys. Rev.* **D54** (1996) 2023; *Nucl. Phys.* **B475** (1996) 47.
[20] Collins J.C., *Nucl. Phys.* **B394** (1993) 169, *and references therein.*
[21] Kretzer S., Phys. Rev. **D62** (2000) 054001; Kniehl B.A., Kramer G., Pötter B., Nucl. Phys. B **582** (2000) 514; Albino S., Kniehl B.A., Kramer G., Nucl. Phys. B **725** (2005) 181; de Florian D., Sassot R., Stratmann M., Phys. Rev. D **76** (2007) 074033; arXiv:0708.0769 [hep-ph].
[22] Adler S.S. *et al.* [PHENIX Collaboration], Phys. Rev. Lett. **91** (2003) 241803.
[23] Abelev B.I. *et al.* (STAR collaboration), Phys. Rev. Lett. **97** (2006) 252001.
[24] Adams J. *et al.* (STAR collaboration), Phys. Rev. Lett. **97** (2006) 152302.
[25] S.S. Adler *et al.* (PHENIX collaboration), Phys. Rev. Lett. **98** (2007) 012002.
[26] Aversa F., Chiappetta P., Greco M., Guillet J.P., Nucl. Phys. B **327** (1989) 105.
[27] Aurenche P. *et al.*, Phys.Lett. B140 (1984) 87; Nucl.Phys. B297 (1988) 661; Baer H., Ohnemus J., Owens J.F., Phys.Rev. D42 (1990) 61; Phys.Lett. B234 (1990) 127; Aurenche P. *et al.*, Phys. Rev. D **73** (2006) 094007.
[28] Gordon L.E. and Vogelsang W., Phys. Rev. **D48** (1993) 3136; *ibid.* D **50** (1994) 1901.
[29] Jäger B., Schäfer A., Stratmann M., Vogelsang W., Phys. Rev. **D67** (2003) 054005.
[30] de Florian D., Phys. Rev. **D67** (2003) 054004.
[31] Jäger B., Stratmann M., Vogelsang W., Phys. Rev. D **70** (2004) 034010.
[32] Contogouris A.P., Kamal B., Merebashvili Z., Tkachov F.V., *Phys. Lett.* **B304** (1993) 329; *Phys. Rev.* **D48** (1993) 4092; Contogouris A.P., Merebashvili Z., *Phys. Rev.* **D55** (1997) 2718; Frixione S., Vogelsang W., *Nucl. Phys.* **B568** (2000) 60; de Florian D., Frixione S., Signer A., Vogelsang W., *Nucl. Phys.* **B539** (1999) 455; Bojak I., Stratmann M., *Phys. Rev.*

D67 (2003) 034010; Jäger B., Kretzer S., Stratmann M., Vogelsang W., *Phys. Rev. Lett.* **92** (2004) 121803.
[33] Ratcliffe P.G., Nucl. Phys. **B223** (1983) 45; Weber A., Nucl. Phys. **B382** (1992) 63; Kamal B., Phys. Rev. **D57** (1998) 6663; Gehrmann T., Nucl. Phys. **B534** (1998) 21; Ravindran V., Smith J., van Neerven W.L., Nucl. Phys. **B647** (2002) 275.
[34] Bland L.C. *et al.*, *Eur. Phys. J.* **C43** (2005) 427.
[35] Adare A. *et al.* [PHENIX Collaboration], Phys. Rev. D **76** (2007) 051106.
[36] Abelev B.I. *et al.* [STAR Collaboration], arXiv:0710.2048 [hep-ex].
[37] Glück M., Reya E., Stratmann M., Vogelsang W., *Phys. Rev.* **D63** (2001) 094005.
[38] Altarelli G., Ross G.G., *Phys. Lett.* **B212** (1988) 391; Altarelli G., Stirling W.J., *Part. World* **1** (1989) 40; Carlitz R.D., Collins J.C., Mueller A.H., *Phys. Lett.* **B214** (1988) 229.
[39] Bourrely C., Soffer J., Phys. Lett. **B314** (1993) 132; Nucl. Phys. **B423** (1994) 329; Chiappetta P., Soffer J., Phys. Lett. **B152** (1985) 126.
[40] Nadolsky P. and Yuan C.P., *Nucl. Phys.* **B666** (2003) 3; *Nucl. Phys.* **B666** (2003) 31.
[41] Stratmann M., talk presented at the "14th International Workshop on Deep Inelastic Scattering (DIS 2006)", Tsukuba, Japan, April 20-24, 2006.
[42] Asymmetry Analysis Collaboration, Hirai M., Kumano S., Saito N., *Phys. Rev.* **D74** (2006) 014015.
[43] de Florian D., Navarro G.A., Sassot R., *Phys. Rev.* **D71** (2005) 094018; Navarro G.A., Sassot R., *Phys. Rev.* **D74** (2006) 011502.
[44] Stratmann M. and Vogelsang W., *Phys. Rev.* **D64** (2001) 114007.
[45] for review, see: Barone V., Drago A., Ratcliffe P.G., Phys. Rept. **359** (2002) 1.
[46] Jaffe R.L. and Ji X., Phys. Rev. Lett. **67** (1991) 552 (1991); Nucl. Phys. **B375** (1992) 527; Artru X. and Mekhfi M., Z. Phys. **C45** (1990) 669 (1990).
[47] Collins J.C., Nucl. Phys. **B396** (1993) 161.
[48] Abe K. *et al.* [Belle Collaboration], Phys. Rev. Lett. **96** (2006) 232002; Ogawa A., Grosse Perdekamp M., Seidl R.C., Hasuko K. [Belle Collaboration], AIP Conf. Proc. **915** (2007) 575.
[49] Anselmino M. *et al.*, Phys. Rev. D **75** (2007) 054032.
[50] Martin O. *et al.*, Phys. Rev. D **57** (1998) 3084; Phys. Rev. D **60** (1999) 117502.
[51] GSI-PAX Collab., Lenisa P. and Rathmann F. (spokespersons) *et al.*, Technical Proposal, arXiv:hep-ex/0505054; arXiv:hep-ex/0412078.
[52] Anselmino M. *et al.*, Phys. Lett. **B594** (2004) 97;
Efremov A.V., Goeke K., Schweitzer P., Eur. Phys. J. **C35** (2004) 207.
[53] Vogelsang W., Phys. Rev. **D57** (1998) 1886, references therein.
[54] Sterman G., Nucl. Phys. **B281** (1987) 310;
Catani S. and Trentadue L., Nucl. Phys. **B327** (1989) 323; *ibid.* **B353** (1991) 183.
[55] Shimizu H., Sterman G., Vogelsang W., Yokoya H., Phys. Rev. **D71** (2005) 114007.
[56] Mukherjee A., Stratmann M., Vogelsang W., Phys. Rev. D **72** (2005) 034011.
[57] Adams J. *et al.* [STAR Collaboration], *Phys. Rev. Lett.* **92** (2004) 171801; Gagliardi C.A. [STAR Collaboration], arXiv:hep-ex/0607003.
[58] Videbaek F. [BRAHMS Collaboration], AIP Conf. Proc. **842** (2006) 401; Lee J.H. and Videbaek F. [BRAHMS Collaboration], AIP Conf. Proc. **915** (2007) 533.
[59] Adler S.S. [PHENIX Collaboration], *Phys. Rev. Lett.* **95** (2005) 202001; Aidala C.A., Ph.D. Thesis, Columbia U. 2006 arXiv:hep-ex/0601009.
[60] for reviews, see: Anselmino M., Efremov A., Leader E., *Phys. Rept.* **261** (1995) 1; E:**281** (1997) 399; Liang Z.T. and Boros C., *Int. J. Mod. Phys.* **A15** (2000) 927.
[61] Sivers D.W., *Phys. Rev.* **D41** (1990) 83; *Phys. Rev.* **D43** (1991) 261.
[62] Efremov E.V. and Teryaev O.V., *Sov. J. Nucl. Phys.* **36** (1982) 140 [*Yad. Fiz.* **36** 242]; *Phys. Lett.* **B150** (1982) 383.

[63] Qiu J.W. and Sterman G., *Phys. Rev. Lett.* **67** (1991) 2264; *Nucl. Phys.* **B378** (1992) 52; *Phys. Rev.* **D59** (1999) 014004.
[64] Eguchi E., Koike Y., Tanaka K., Nucl. Phys. B **763** (2007) 198; Koike Y. and Tanaka K., Phys. Lett. B **646** (2007) 232; Phys. Rev. D **76** (2007) 011502.
[65] Kanazawa Y. and Koike Y., *Phys. Lett.* **B478** (2000) 121; *Phys. Rev.* **D64** (2001) 034019.
[66] Anselmino M., Boglione M., Murgia F., *Phys. Lett.* **B362** (1995) 164; Anselmino M. and Murgia F., *Phys. Lett.* **B442** (1998) 470; D'Alesio U. and Murgia F., *Phys. Rev.* **D70** (2004) 074009; Anselmino M., D'Alesio U., Melis S., Murgia F., *Phys. Rev. D* **74** (2006) 094011; A. Bacchetta *et al.*, arXiv:hep-ph/0703153.
[67] Kouvaris C., Qiu J.W., Vogelsang W., Yuan F., Phys. Rev. D **74** (2006) 114013.
[68] Collins J.C. and Soper D.E., *Nucl. Phys.* **B193** (1981) 381; E:**B213** (1983) 545; *Nucl. Phys.* **B197** (1982) 446; *Nucl. Phys.* **B194** (1982) 445.
[69] Collins J.C., Soper D.E., Sterman G., *Nucl. Phys.* **B250** (1985) 199.
[70] Ji X., Ma J.P., Yuan F., *Phys. Rev.* **D71** (2005) 034005; *Phys. Lett.* **B597** (2004) 299.
[71] Collins J.C. and Metz A., *Phys. Rev. Lett.* **93** (2004) 252001.
[72] Ji X., Qiu J.W., Vogelsang W., Yuan F., *Phys. Rev. Lett.* **97** (2006) 082002; *Phys. Rev.* **D73** (2006) 094017; *Phys. Lett.* **B638** (2006) 178.
[73] Kane G.L., Pumplin J., Repko W., *Phys. Rev. Lett.* **41** (1978) 1689.
[74] Brodsky S.J., Hwang D.S., Schmidt I., *Phys. Lett.* **B530** (2002) 99; *Nucl. Phys.* **B642** (2002) 344.
[75] Collins J.C., *Phys. Lett.* **B536** (2002) 43.
[76] Ji X. and Yuan F., *Phys. Lett.* **B543** (2002) 66; Belitsky A.V., Ji X., Yuan F., *Nucl. Phys.* **B656** (2003) 165.
[77] Ji X.D., Ma J.P., Yuan F., *Nucl. Phys.* **B652** (2003) 383.
[78] Burkardt M., *Phys. Rev.* **D74** (2006) 013002; *Phys. Lett.* **B639** (2006) 462; Burkardt M. and Schnell G., Phys. Rev. D **74** (2006) 013002.
[79] Burkardt M., *Phys. Rev. D62* (2000) 071503; *Phys. Rev.* **D66** (2002) 114005; *Int. J. Mod. Phys.* **A18** (2003) 173; *Nucl. Phys.* **A735** (2004) 185; *Phys. Rev.* **D72** (2005) 094020.
[80] Burkardt M. and Hwang D.S., *Phys. Rev.* **D69** (2004) 074032; Ralston J.P., Pire B., *Phys. Rev.* **D66** (2002) 111501; Diehl M., *Eur. Phys. J.* **C25** (2002) 223; E: *Eur. Phys. J.* **C31** (2003) 277; Belitsky A.V., Müller D., *Nucl. Phys.* **A711** (2002) 118; Ji X.D., *Phys. Rev. Lett.* **91** (2003) 062001; Belitsky A.V., Ji X.D., Yuan F., *Phys. Rev.* **D69** (2004) 074014; Diehl M. and Hägler P., *Eur. Phys. J.* **C44** (2005) 87; Avakian H. *et al.*, arXiv:0709.3253 [hep-ph].
[81] Bland L.C. *et al.*, "Transverse-Spin Drell-Yan Physics at RHIC", `http://spin.riken.bnl.gov/rsc/write-up/dy_final.pdf`
[82] Boer D., Mulders P.J., Pijlman F., *Nucl. Phys.* **B667** (2003) 201.
[83] Boer D. and Vogelsang W., *Phys. Rev.* **D69** (2004) 094025.
[84] Vogelsang W. and Yuan F., *Phys. Rev.* **D72** (2005) 054028.
[85] Bomhof C.J., Mulders P.J., Pijlman F., *Phys. Lett.* **B596** (2004) 277; Bacchetta A., Bomhof C.J., Mulders P.J., Pijlman F., *Phys. Rev.* **D72** (2005) 034030; Bomhof C.J., Mulders P.J., Pijlman F., *Eur. Phys. J.* **C47** (2006) 147; Bomhof C.J. and Mulders P.J., JHEP **0702** (2007) 029; arXiv:0709.1390 [hep-ph].
[86] Collins J.C. and Qiu J.W., Phys. Rev. D **75** (2007) 114014.
[87] Qiu J.W., Vogelsang W., Yuan F., Phys. Lett. B **650** (2007) 373; Phys. Rev. D **76** (2007) 074029.
[88] Vogelsang W. and Yuan F., Phys. Rev. D **76** (2007) 094013.
[89] Abelev B.I. *et al.* [STAR Collaboration], Phys. Rev. Lett. **99** (2007) 142003.